

Supplementary Materials for

Tip-enhanced strong coupling spectroscopy, imaging, and control of a single quantum emitter

Kyoung-Duck Park*, Molly A. May, Haixu Leng, Jiarong Wang, Jaron A. Kropp,
Theodosia Gougousi, Matthew Pelton*, Markus B. Raschke*

*Corresponding author. Email: markus.raschke@colorado.edu (M.B.R.); mpelton@umbc.edu (M.P.);
kyoungduck.park@colorado.edu (K.-D.P.)

Published 12 July 2019, *Sci. Adv.* **5**, eaav5931 (2019)
DOI: 10.1126/sciadv.aav5931

This PDF file includes:

Section S1. Characterization of single isolated QDs
Section S2. Lorentzian fitting of emission spectra of uncoupled QD and cavity
Section S3. A coupled oscillator model for plexciton spectra
Section S4. Parameters of model fit
Section S5. FEM simulation of strong coupling
Section S6. FDTD simulation of optical field distribution in a plasmonic cavity
Fig. S1. AFM image of QDs on Au substrate.
Fig. S2. Lorentzian line fit of PL spectra.
Fig. S3. FEM simulation of scattering spectra.
Fig. S4. 3D FDTD simulation of the optical field enhancement.
References (58–60)

Section S1. Characterization of single isolated QDs

In our experiment, the 8 nm CdSe/ZnS quantum dots (QDs) were dispersed and isolated on the sample substrate by optimizing dilution factor and drop casting time. We diluted the raw solution (900249-1ML, Sigma Aldrich) by 20,000 times. We then drop casted the diluted solution (20 μ l) onto Au substrate for 10 s. The optimized QD samples on Au substrate were measured using a tapping mode atomic force microscope (AFM, Dimension 3100, Park Systems) to investigate QD density. Through a series of measurement for different samples (different drop casting) and different spots in the same sample, we verified the density of the QDs on the surface was \sim 5 dots in a 1 μ m by 1 μ m window as a form of single QD. Figure S1 shows one the AFM topography images. The average height of QDs was 8.0 nm \pm 0.9 nm in a series of AFM images.

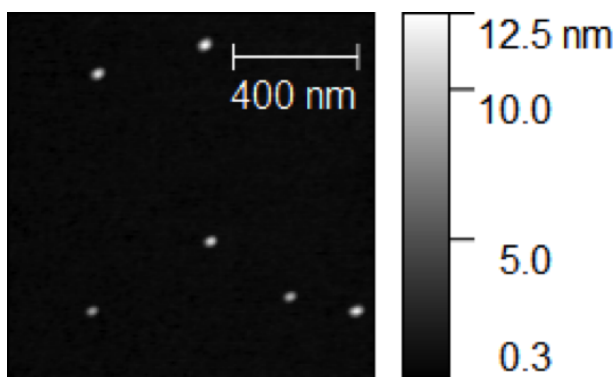


Fig. S1. AFM image of QDs on Au substrate. The well-dispersed quantum dots have an average height of 8.0 nm \pm 0.9 nm.

Section S2. Lorentzian fitting of emission spectra of uncoupled QD and cavity

In Fig. 2A of the main text, we show PL spectra of the QD exciton and the gap plasmon as an uncoupled state of emitter and cavity. We perform Lorentzian line fit analysis of these PL spectra to derive the peak energy and spectral linewidth of them as shown in fig. S2A and fig. S2B. The derived peak energies ($\omega_{QD} = 1.856$ eV and $\omega_{SP} = 1.912$ eV) and linewidths ($\gamma_{QD} = 0.097 \pm 0.002$ eV and $\gamma_{SP} = 0.126 \pm 0.002$ eV) of these emission spectra are used as parameters in our theoretical model (Eq. 1). Since the peak energy and linewidth of these spectra can be varied due to the spectral diffusion of QD and resonance shift of cavity with respect to the gap size, the fit parameters are slightly modified in the model for the best fitting.

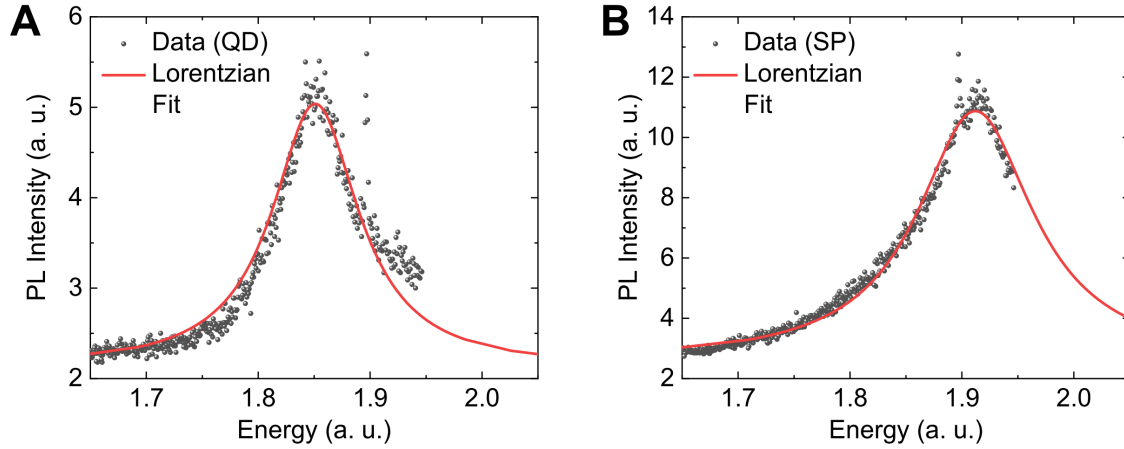


Fig. S2. Lorentzian line fit of PL spectra. PL spectra of the QD exciton (a) and the gap plasmon (b) with Lorentzian line fit analysis, derived from Fig. 2A.

Section S3. A coupled oscillator model for plexciton spectra

The model used for fitting the TEPL spectra (Fig. 2, Fig. 3, and Fig. 4) is derived in Ref. (33) by starting from the interaction Hamiltonian for a quantized radiation field interacting with a two-level emitter located at the antinode of the field in an optical microcavity and allowing side and forward emissions to the surrounding heat reservoir. The dipole approximation and the rotating wave approximation are applied and the evolution of the probability amplitudes for each possible state with one excitation in the system are obtained using the Weisskopf-Wigner approximation, which assumes that the state vector of the system does not depend on those at previous times. In the strong coupling approximation, this yields the generalized vacuum Rabi frequency used to derive Eq. 2 in the main text. Finally, assuming that the emitter is prepared in an excited state at time $t = 0$ and using the Weiner-Khintchine theorem which in this case and yields Eq. 1 of the main text. Anticrossing curves were generated by solving this equation to find its normal modes which follow Eq. S1.

$$\omega_{\pm} = \frac{\omega_{QD} + \omega_{SP}}{2} - \frac{i}{4}(\gamma_{QD} + \gamma_{SP}) \pm \sqrt{(g/2)^2 + \frac{1}{4}\left(\omega_{SP} - \omega_{QD} - i\frac{\gamma_{QD} - \gamma_{SP}}{2}\right)^2} \quad (1)$$

Section S4. Parameters of model fit

Table S1. Parameters of model fit for TEPL spectra in Fig. 2A and Fig. 3A of the main text.

	Fig. 2A SC, eV	Fig. 3A SC 1, eV	Fig. 3A SC 2, eV	Fig. 3A SC 3, eV	Fig. 3A SC 4, eV
ω_{SP}	1.847	1.800	1.822	1.827	1.800
γ_{SP}	0.148	0.176	0.164	0.158	0.085
ω_{QD}	1.843	1.870	1.840	1.842	1.856
γ_{QD}	0.092	0.065	0.050	0.050	0.110
g	0.143	0.163	0.153	0.141	0.070

Table S2. Parameters of model fit for TEPL spectra in Fig. 4A of the main text.

	Fig. 4A 0 nm, eV	Fig. 4A 7.5 nm, eV	Fig. 4A 15 nm, eV	Fig. 4A 22.5 nm, eV
ω_{SP}	1.840	1.848	1.850	1.840
γ_{SP}	0.175	0.180	0.180	0.180
ω_{QD}	1.859	1.859	1.859	1.861
γ_{QD}	0.031	0.031	0.031	0.031
g	0.150	0.149	0.141	0.137

Table S3. Parameters of model fit for TEPL spectra in Fig. 4B of the main text.

	Fig. 4B 0 nm, eV	Fig. 4B 1 nm, eV	Fig. 4B 2 nm, eV	Fig. 4B 3 nm, eV
ω_{SP}	1.841	1.854	1.866	1.840
γ_{SP}	0.140	0.140	0.128	0.128
ω_{QD}	1.859	1.859	1.861	1.861
γ_{QD}	0.060	0.060	0.045	0.060
g	0.137	0.116	0.091	0.088

Section S5. FEM simulation of strong coupling

Rigorous electromagnetic simulations of the plexciton scattering spectra, which are qualitatively equivalent to PL spectra in the strong coupling regime (43), were performed using the finite element method (FEM) in COMSOL, as shown in Fig. 2D. While many simulations approximate emitters as point dipoles, these simulations treat the QD as a dielectric particle with realistic dimensions based on its ground-state transition following the work of Wu et al. (37) and the nano-antenna is approximated as a finite length ellipsoid with a 5 nm radius of curvature.

The simulation used realistic parameters for the geometry and dielectric functions. For the QD, the dielectric constant is in a form of Lorentz model, with $\epsilon = 5$, $\omega_0 = 1.82$ eV, $\gamma_0 = 0.05$ eV and $f = 0.8$ (oscillator strength). The gold dielectric function is from Rakic et al (58). We use the wave-optics module of COMSOL with the electric field polarized perpendicular to the Au film. The simulation is done in two parts, first, the simulation runs without the gold nanoparticle to calculate the field. The second run includes the gold nanoparticle and calculated the scattered field by subtracting the field from the first run. The simulation takes around 2 hours on our workstation (20 cores Intel Xeon).

The simulated spectra were fit using the same analytical model that was used to fit the measured PL spectra and shows excellent agreement with the measured data for both the coupled system and the plasmon response with no QD present as shown in Fig. 2D.

Figure S3 shows FEM simulation of scattering spectra for a QD for a range of oscillator strength values ($f = 0$ to 1.2). For the simulations with $f < 0.6$, the mode energy of the upper polariton is close to the SPP resonance, but with asymmetric spectral shape. In contrast, when $f > 0.6$, the Rabi frequency increases with the larger scattering cross-section of the lower polariton near the QD resonance as expected. The oscillator strength of QD is associated with the orientation of TDM in our experiment which gives rise to variation in the coupling strength

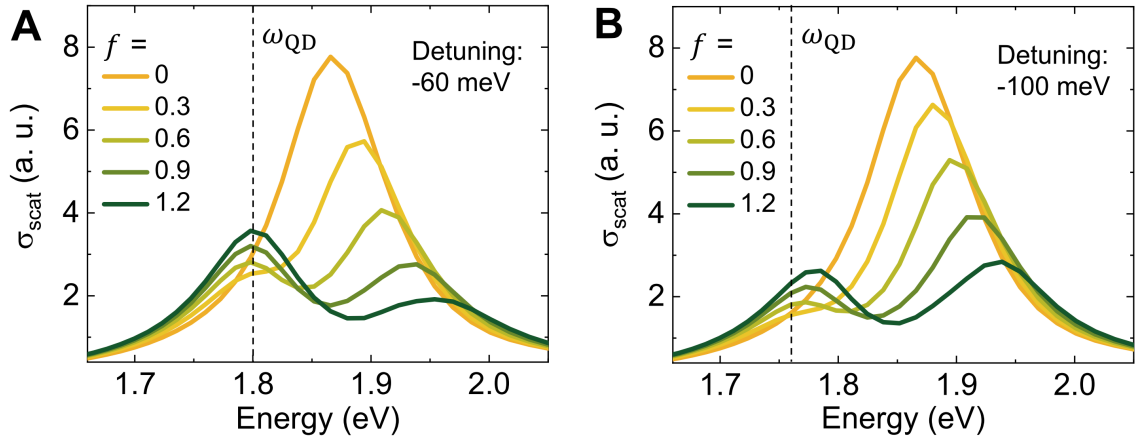


Fig. S3. FEM simulation of scattering spectra. Finite element method (FEM) simulation of scattering spectra for a QD with detuning of -60 meV (A) and -100 meV (B) for increasing oscillator strengths (f).

as shown in Fig. 3A. While we set the detuning parameter near 0 meV for the simulation of Fig. 2D, we set detuning of -60 meV and -100 meV in fig. S3 to demonstrate that the measured strong coupling over a large detuning range is also in good agreement with electrodynamic simulation.

Section S6. FDTD simulation of optical field distribution in a plasmonic cavity

To characterize the local optical field enhancement and the mode volume of the plasmonic nano-cavity, we calculate the optical field distribution using 3D finite-difference time-domain (FDTD) simulations (Lumerical Solutions, Inc.) for our experimental conditions. A CdSe/ZnS QD and a 0.5 nm dielectric capping layer (Al_2O_3) are modelled with established optical properties (n , k) and realistic dimensions. Figure S4B and fig. S4D show the out-of-plane optical field ($|\mathbf{E}_z|$) map for the different excitation polarization condition as shown in fig. S4A and fig. S4C. 3D FDTD simulations show that excitation polarization parallel to the tip (fig. S4B) gives rise to an ~ 800 -fold field intensity enhancement compared to polarization perpendicular to the tip (fig. S4D).

The $|\mathbf{E}_z|$ mode is most strongly bound in sub-nm dielectric gap between tip and QD, as also can be seen in Fig. 1B. The idea of using a dielectric gap between the plasmonic structure and the semiconductor is motivated by a recently demonstrated design of plasmonic nanowire lasers (59, 60). In these studies, a 1D semiconductor nanowire sits on a 2D metallic surface with a nanoscale gap created by a dielectric layer. In the dielectric layer, the strongly confined plasmon mode enhances the radiative recombination rate through the Purcell effect in the weak coupling regime. Moreover, the spontaneously emitted light is confined in this gap and propagates along the dielectric waveguide as a form of polariton mode. In our design, the plasmon mode is squeezed much stronger in a 0.5 nm thickness dielectric layer between the 0D structures of semiconductor (QD) and plasmonic tip which gives rise to plexciton photoluminescence (PL) emission in the strong coupling regime. Here we take advantage of the tilted tip approach to increase the field enhancement by suppressing the overdamped resonance of a conventional surface-normal oriented tip (29).

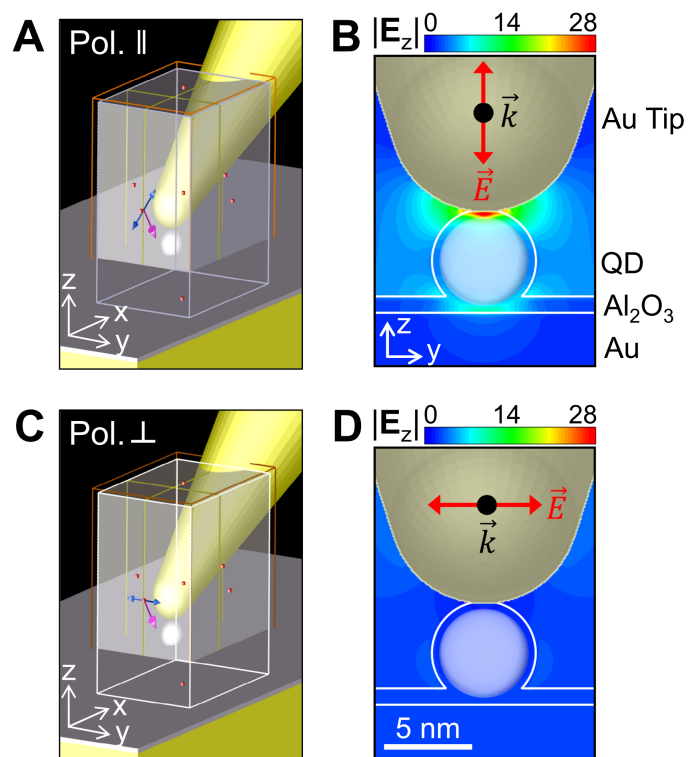


Fig. S4. 3D FDTD simulation of the optical field enhancement. (A, C) Schematic of modelling consists of the tilted Au tip, CdSe/ZnS quantum dot, Al₂O₃ dielectric layer, and Au substrate with incident light (632.8 nm) polarization parallel to the tip axis (experimental conditions of Fig. 1A). (B, D) The out-of-plane optical field ($|E_z|$) map for the experimental conditions of (A) and (C).